Modeling and visualization of uncertainties of categorical spatial data using geostatistics, 3D planar projections and color fusion techniques

Carlos Alberto Felgueiras[1], Jussara de Oliveira Ortiz[1], Eduardo Celso Gerbi Camargo[1], Laércio Massaru Namikawa[1], Thales Sehn Korting[1]

[1]Instituto Nacional de Pesquisas Espaciais (INPE)
Caixa Postal 515 – 12227-010 – São José dos Campos – SP – Brazil

{carlos,jussara,eduardo,laercio,tkorting}@dpi.inpe.br

Abstract. *This article explores the uncertainty modelling and their different ways of visualizations for categorical spatial attributes. It shows how to model these attributes using procedures of indicator geostatistics. The geostatistical modelling uses as input a set of sample points of the categorical attribute that are transformed in indicator samples according the classes of interest. Experimental and theoretical semivariograms of the indicator fields are defined representing the spatial variation of the indicator information. The indicator fields, along with their semivariograms, are used to determine the uncertainty model, the conditioned probability distribution function, of the attribute at any location inside the geographic region delimited by the samples. The probability functions are used for producing prediction and uncertainty maps based on the maximum class probability criterion. These maps can be visualized using different techniques. In this work, it is considered individual visualization of the predicted and uncertainty maps and of the predictions combined with their uncertainties. The combined visualizations are based on 3D planar projection and on the Red-Green-Blue to Intensity-Hue-Saturation (RGB-IHS) fusion transformation techniques. The methodology of this article is illustrated by a case study with real data, a sample set of soil textures observed in an experimental farm located in the region of São Carlos city in São Paulo State, Brazil. The resulting maps of this case study are presented and the advantages and the drawbacks of the visualization options are analyzed and discussed.*

Resumo. *Este artigo explora a modelagem de incerteza e suas diferentes formas de visualização para atributos espaciais categóricos. Utilizam-se procedimentos geoestatísticos por indicação para a modelagem dos atributos. Essa modelagem usa, como dados de entrada, um conjunto de amostras pontuais do atributo categórico que são transformadas em amostras por indicação de acordo com as classes de interesse. Para cada amostra por indicação obtém-se semivariogramas experimentais e teóricos representando a variação espacial da informação por indicação. Os campos por indicação, em conjunto com seus respectivos semivariogramas, são usados para obtenção do modelo de incerteza, a função de distribuição de probabilidade condicionada às amostras, do atributo em qualquer localização espacial dentro da região geográfica delimitada pelo conjunto amostral. As funções de distribuição de probabilidades possibilitam a produção de mapas de predições e incertezas utilizando-se informação da moda, classe de máxima probabilidade, da*

distribuição. Esses mapas podem ser visualizados utilizando-se diferentes técnicas. Neste trabalho consideraram-se visualizações individuais e combinadas dos mapas de predições e de suas respectivas incertezas. As visualizações combinadas basearam-se em projeções planares tridimensionais e nas técnicas de fusão por transformações no espaço de cores conhecidas como RGB-IHS ("Red, Green and Blue" to "Intensity, Hue and Saturation") e vice-versa. A metodologia apresentada neste artigo é ilustrada por um estudo de caso com dados reais, um conjunto amostral de texturas de solo observado em uma fazenda experimental localizada na cidade de São Carlos, em São Paulo, Brasil. Os mapas resultantes desse estudo de caso são apresentados e as vantagens e desvantagens das opções de visualização são analisadas e discutidas.

1. Introduction

For many environmental applications, continuous or categorical spatial attributes can be computationally modelled from a set of sample points obtained, on field works for example, in a geographical region of interest. The attribute representations are used as input for spatial modelling functions whose outputs simulate Earth related phenomena, in a Geographical Information System (GIS) database, allowing deeper studies and analyses to support better decision makings in real world problems.

Associated with the produced results always there will be an uncertainty, which is distributed spatially within the geographical region. Geostatistical approaches yield tools for representing the stochastic local or global uncertainties of geographical attributes from their sample sets. Maps of predictions, such as mean, median or mode values, and related uncertainty maps, based on standard deviation, quantile or probability values, can be extracted from the attribute uncertainty models. So, the predictions are accompanied with their uncertainties that are also spatially distributed in the region of interest. In special, using indicator geostatistical functions for interpolations and simulations, the uncertainty fields take into account the sample values and also their relative spatial locations (Deutsch and Journel (1998)). Moreover, the indicator geostatistics allow to model uncertainties of categorical, besides the continuous, attribute information (Goovaerts (1997) and Felgueiras et al. (2015)).

A significant topic for the attribute representations is to visualize their uncertainty fields in a way that facilitates the analyses of the spatial distribution in terms of quality of the attribute modelling. Many articles have addressed the subject of visualization methods to represent spatial data uncertainties (Pebesma et al. (2007), Tan and Chen (2008), Sun and Wong (2010), Senaratne et al. (2012) and Kinkeldey et al. (2014)). Typically, an attribute uncertainty map is visualized separated from the data map using a gray scale look up table where the minimum and maximum values are assigned to the black and white colors respectively, or vice-versa. The intermediary colors are defined as midway gray levels proportional to the attribute values. It is common, also, to show the uncertainty map using different color tables, as the rainbow colors for example.

Koo (2015) presents a framework for combining visual variables to simultaneously represent an attribute and its uncertainty. The author uses three categories

of uncertainty visualizations: coloring, overlap symbols and integrate symbols. Another interesting approach is to use a fusion technique to visualize the attribute data merged with the uncertainty displaying both information integrated in a single map. Hengl (2003) describes two methods for visualization of uncertainty associated with predictions of continuous and categorical variables. Both methods are based on the Intensity-Hue-Saturation (IHS) color model with uncertainty coded with whiteness. Also, in a GIS environment, it is common to obtain 3D planar projections of attribute representations and to use the uncertainty as the texture of the rendered images.

In this context, the objective of this article is to explore the modelling and visualization the uncertainties of categorical spatial attributes. The uncertainty modelling is performed by procedures of indicator geostatistics applied to a sample set of points of a spatial categorical attribute. It is considered individual visualization of the uncertainty maps, visualization of the predictions combined with their uncertainties using 3D planar projections and visualization resulting from fusion technique based on Red-Green-Blue to Intensity-Hue-Saturation (RGB-IHS) color transformation. The methodology is illustrated with a case study developed for a sample set of soil texture observed in an experimental farm located in the region of São Carlos city in São Paulo State, Brazil. Four classes of soil texture, namely Sandy, Medium Clayey, Clayey and Too Clayey, are considered in order to obtain the predictions along with their uncertainties. The resulting maps of this case study are presented and analyzed and the advantages and the drawbacks of the visualization options are discussed

The organization of this article starts with this introduction section. Section 2 presents summaries of the main concepts linked to the main issues of this article. Section 3 addresses the methodology of this work while section 4 describes the case study used to illustrate the modelling and visualizations resulting from application of the proposed methodology. Section 5 shows results and analyses related to the adopted attribute uncertainty modelling and map visualizations. In the section 6 important conclusions are reported along with suggestions for future works.

2. Concepts

2.1. Indicator Geostatistics

Geostatistical procedures can be used to generate statistical uncertainty models of spatial attributes and, from them, to derive attribute realizations, predictions (such as mean, median and mode values) and uncertainty metrics based on probabilities and confidence intervals of standard deviations and quantiles.

The geostatistical indicator approaches allow for modeling the joint conditional distribution functions of continuous or categorical random variables, at any unknown spatial location **u**, considering an available set of sample points. The Simulation process consists of drawing realizations from the joint conditional distribution functions.

For a categorical variable, its conditional probability distribution function (*cpdf*) is built from estimations on indicator fields obtained by indicator transformations applied to the original sample set, of *nsamples*, $\{z(\mathbf{u}_j), j = 1, ..., n_{samples}\}$, considering any number of *nclasses*. Instead of the variable $Z(\mathbf{u}_j)$, consider its binary indicator transformation $I(\mathbf{u}_j; k)$, as defined by the relation of Equation 1.

$$I(\mathbf{u}_j; k) = \begin{cases} 1, & \text{if } Z(\mathbf{u}_j) = k \\ 0, & \text{otherwise} \end{cases} \quad (1)$$

This transformation is equivalent to associate probability 1 (100%) for $Z(\mathbf{u}_j)$ values which are equal to class k and 0 otherwise. The result of transformation expressed in Equation (1) generates k indicator fields, with 0 and 1 values, $\{i(\mathbf{u}_j), j = 1, ..., n_{samples}\}$ of the indicator variable $I(\mathbf{u}_j; k)$. Next, experimental indicator semivariograms are defined, from the Equation 2, for each one of the k indicator fields to represent their spatial variations.

$$\hat{\gamma}_{(\mathbf{h},k)} = \frac{1}{2\mathrm{N}(\mathbf{h})} \sum_{j=1}^{\mathrm{N}(\mathbf{h})} \left[i(\mathbf{u}_j; k) - i(\mathbf{u}_j + \mathbf{h}; k) \right]^2 \quad (2)$$

where $i(\mathrm{u_j}; k)$ and $i(\mathrm{u_j} + \mathbf{h}; k)$ are the j-th values of the indicator variable I separated by the distance vector $\mathbf{h}$, and $\mathrm{N}(\mathbf{h})$ is the number of the pairs points that are separated by $\mathbf{h}$.

The k indicator fields and their respective theoretical semivariograms are used by the kriging procedure for assessment of class probabilities at any spatial location inside the region of interest. Moreover, the sequential indicator simulation procedure uses kriging, applied on the indicator sample and pre-realization values, in order to infer the *cpdfs* and the class realizations of the categorical variable (Goovaerts (1997) and (2001)). Maps of predictions with $c^*(\mathbf{u}_\alpha)$ and uncertainties $Unc^*(\mathbf{u}_\alpha)$ values, based on local maximum probabilities $P_k(\mathbf{u}_\alpha)$ of any *cpdf*, can be evaluated from the set of realization fields as presented by the Equations 3 and 4.

$$c^*(\mathbf{u}_\alpha) = \mathrm{c}_l(\mathbf{u}_\alpha) \text{ where } P\left(\mathrm{c}_l(\mathbf{u}_\alpha)\right) > P\left(\mathrm{c}_k(\mathbf{u}_\alpha)\right) \quad \forall\, l, k = 1, \ldots, nclasses \quad (3)$$

$$Unc^*(\mathbf{u}_\alpha) = 1 - Max\left(P\left(\mathrm{c}_k(\mathbf{u}_\alpha)\right)\right) \quad k = 1, \ldots, nclasses \quad (4)$$

In Equations 3 and 4, $\mathbf{u}_\alpha$, $\{\alpha = 1,...,gridsize(n_{lines} \text{ x } n_{columns})\}$, are spatial locations regularly distributed in the geographic space, determining regular grid representation structures.

2.2. 3D Planar Projection

The 3D planar projections allow the visualization of 3D information in a 2D surface using geometric transformations. Parallel projections position the viewpoint at the infinite while when the viewpoint is elsewhere the projections are known as perspective projections. The 3D planar projections are generally based on applying geometric transformations based on Translations, Scaling and Rotations. Many books of basic computer graphics, such as Newman and Sproul (1979) and Foley et al. (1985) present details of the mathematics evolved on this subject. Rendering planar projections of 3D information considers hidden lines or surfaces and inclusion of additional 2D texture information to get more realistic 2D images.

2.3. RGB - IHS Transformations

The human eye perceives color information through three types of cones with sensitivity to the Red (R), Green (G) and Blue (B) wavelengths of visible electromagnetic energy. This physical schema is the base of the RGB color system, where individual intensities

of Red, Green and Blue combine to define a color. In terms of human perception, it is more natural to evaluate the values Intensity (I), the Hue (H) and the Saturation (S) of a color. Intensity corresponds to the total energy measure involved in all wavelengths, and provides the brightness sensation. The Hue is the average wavelength of the light, and determines the object color. Saturation express the purity of the color with low saturation values producing pale tones and high saturation values presenting pure colors. The IHS color system is also known by other names, depending on how the Intensity component is named: HSV system has Value (V) for Intensity; and HLS has Lightness (L) for Intensity (there is a slight change in this system but the overall idea is the same). More information is available in most Computer Graphics book, including Foley et al. (1985). There are different ways to perform the RGB-IHS transformation, and vice-versa.

The RGB-IHS and IHS-RGB color transformations are widely used in remote sensing applications to fuse images of different resolutions and/or sensors. Three bands from a multispectral image are selected and associated to a corresponding RGB component and then transformed into IHS model. Next, in the IHS-RGB reverse transformation the process replaces one of the IHS components. Usually, the intensity component is replaced by one panchromatic band with higher resolution when a pan-sharpening fusion is required. In this case, the resulting RGB components present an enhanced image with higher spatial resolution with the colors of the multispectral image. In this work, we explore this fusion procedure using the spatial attribute predicted image, as the input multispectral image, and it respective uncertainty as auxiliary information that will replace the Intensity and Saturation components.

3. Methodology

Considering specifically spatial categorical attributes, the methodology adopted in this work, for their uncertainty modelling and visualizations, comprises the following sequence:

- A sampling set of points of the categorical attribute, given as the input data, is initially transformed in indicator sample sets according to the number of classes considered.
- Experimental and theoretical semivariograms are obtained for the indicator sample fields to represent their respective spatial variability.
- The indicator fields and their theoretical semivariograms are used to run Sequential Indicator Simulation (SIS) functions of the Geostatistical Software Library (GSLib) (Deutsch and Journel (1998)), in order to obtain realization values and from them prediction and uncertainty maps of the attribute in the spatial region of interest.
- Prediction and uncertainty maps are visualized individually using different lookup tables.
- Prediction and uncertainty maps are combined in 3D planar projection visualizations.
- The RGB-IHS transformation is applied in the Red, Green and Blue components of the predicted categorical map.
- The IHS-RGB reverse transformation is applied by replacing the Intensity or the Saturation component by the Uncertainty map.

- The RGB layers from the reverse transformation are combined in order to display and compare the results of the fusion processes.).

4. Case Study

In order to illustrate the methodology of this work, a set of points of soil texture data sampled in the region of an experimental farm known as Canchim. The region of interest is located in the city of São Carlos, São Paulo, Brazil, and covers an area of 2660 ha between the north-south coordinates from s 21º54'32'' to s 21º59'39'' and the east-west coordinates from w 47º48'11'' to w 47º51'59''. The input data set consists of 86 samples of soil texture information each classified as one of the following four classes: Sandy, Medium Clayey, Clayey or Too Clayey. Figure 1 illustrates the borders of the Canchim farm and the spatial locations of the classified soil texture samples. This classified map was obtained by nearest neighbor estimations showing regions of influence of each class. The SPRING GIS (Camara et al. (1996)) was used to store, analyze and visualize all the geoinformation of this work.

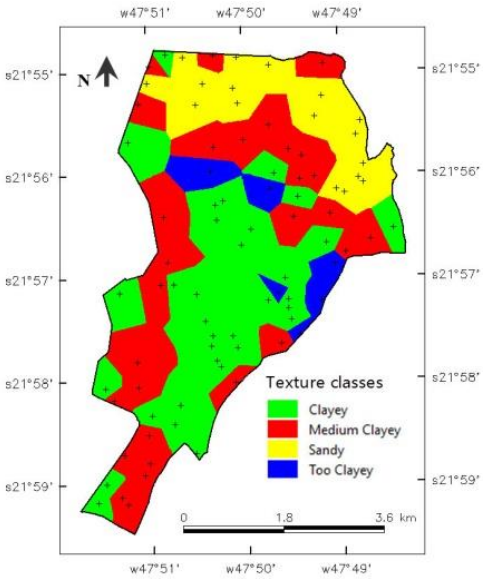

Figure 1: Distribution of the soil texture sample points of the Canchim region.

5. Results and Discussion

5.1. Soil texture estimated by Indicator Geostatistics

The spatial dependence analyses are based on the indicator sample fields of the soil texture classes generated by the indicator transformation as defined in Equation 1. The spatial dependences analyses are represented by the indicator semivariograms generated from the indicator sample set defined by each texture class. The experimental indicator semivariograms were assessed and fitted by theoretical ones in the SPRING GIS computational environment. The indicator semivariogram parameters, along with the global probabilities of each texture class, are reported in Table 1. All semivariograms were fitted with exponential functions. The global probabilities are assessed by the ratio

between the number of samples of each class and the total number. These parameters and the sample set are used as input for the SIS function.

Table 1: Parameters of the indicator semivariograms related to the soil texture classes.

Texture Class	Nugget Effect	Contribution	Range	Global Probability
Sandy	0.00	0.14	1915	0.20
Medium Clayey	0.00	0.22	902	0.35
Clayey	0.01	0.20	1059	0.38
Too Clayey	0.03	0.05	695	0.07

Figure 2(a) shows the map of predicted soil texture classes while the Figure 2(b) shows the map of their uncertainties, where both maps were obtained from the resulting realizations of the GSLib SIS function known as sisim. Those estimations were assessed from the *cpdfs*' higher probability criterion, as defined in Equations 3 and 4, for each spatial location considered.

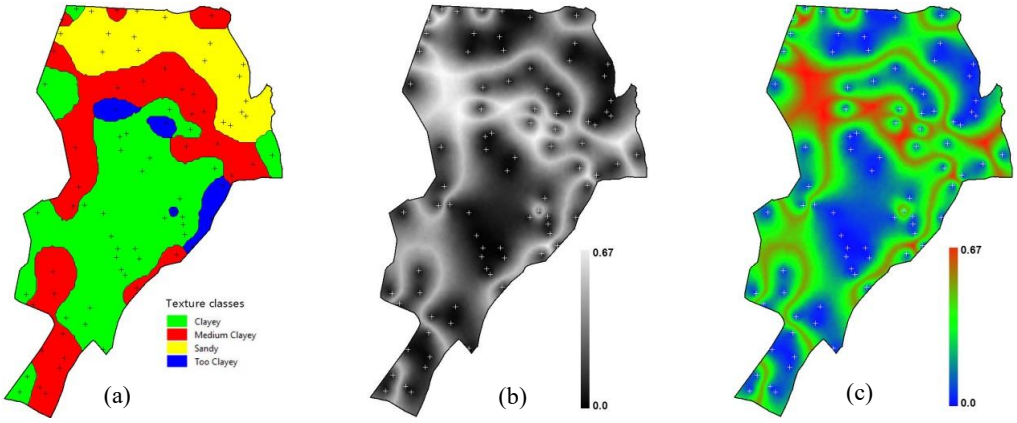

Figure 2: Map of (a) predictions, (b) uncertainties in gray scale color table and (c) uncertainties using a rainbow color table

A qualitative, visual, comparison between the map of predictions of Figure 2(a) and the map of nearest neighbors' interpolation, of Figure 1, shows that the both maps agree with the local information presented in the texture sample set. The differences appear in the smoother class transitions presented in the map predicted from the geostatistical simulated values.

The uncertainties depicted in Figures 2(b) and 2(c), as expected for environmental attributes, are higher in the borders, the transitions areas, of the soil texture class regions. Consequently, the probability uncertainty values are lower in the middle of each map class. It can be observed also that the minimum uncertainty values appear at the sample locations since the geostatistical procedures are exact, i.e., the estimation is equal to the sample value at any sample location.

Figure 2(c) depicts the map of uncertainties using a rainbow look up table color. The map of Figure 2(b), compared with the one of Figure 2(c), seems to be better to emphasize the borders, the transitions between classes where the uncertainties are higher, among the classes of the predicted map. Other lookup tables can be used in order to highlight specific detail.

5.2. Uncertainty visualization by 3D planar projection

Figure 3(a) displays the uncertainty information in a 3D Planar Projection using the gray level map of Figure 2(b) as the texture of the final rendered figure while in the Figure 3(b) the texture was gathered from the predicted map of the Figure 2(a).

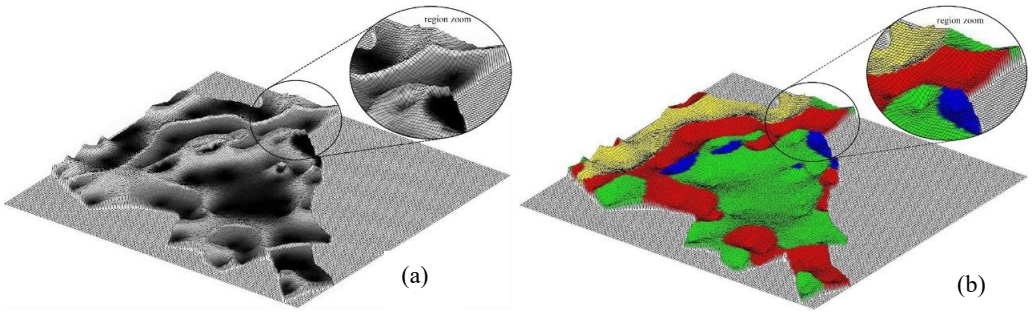

Figure 3: Planar projections of the uncertainty map displayed in (a) gray levels and (b) predicted classes as texture of the rendered map.

Figures 3(a) and 3(b) can be rendered using different azimuth and zenith angles and are considered qualitative applications. These drawings are useful in order to have a visual perception of the vertical variation of the uncertainty information in different angles together with other soil texture information. Other textures can be used, e. g., the one of Figure 2(c).

5.3. Uncertainty Visualization by RGB-IHS fusion

All the images considered in this application are color coded with 8 bits, so the minimum and the maximum values for the colors are 0 and 254. The 255 value is used as the background color. The texture classes have the following R, G, B color composition: Sandy 254, 254, 0 (Yellow); Medium Clayey 254, 0, 0 (Red); Clayey 0, 254, 0 (Green) and; Too Clayey 0, 0, 254 (Blue). Considering its class colors, the predicted texture map can be decomposed in three new maps corresponding to the Red, Green and Blue components.

Applying the RGB-IHS transformation in the components of the RGB texture map results in a Saturation component equal to 254, the maximum value, for the entire region. The Intensity component was assigned to 127, a medium value. The Hue component varies according the colors presented in the predicted map. Low Hue values (Black) represents the yellow color, low medium values the Green, high medium values the Blue and high values the Red. Figure 4 depicts the results of the IHS-RGB transformation replacing (a) the Intensity and (b) the Saturation by the Uncertainty map of Figure 2(b).

In Figure 4(a), the original colors of the predicted map tend to darker colors where the uncertainty is very low. This occurs because any color with low intensity appears as

black. To avoid the dark colors, one could remap the uncertainty interval values to higher values. In any case the map of Figure 4(a) shows the predominant colors of each class going from low intensities, where uncertainties are low, to high intensities, where uncertainties are high.

The map of Figure 4(b) has similar behavior as the one in Figure 4(a) when the Saturation is replaced instead of the Intensity. In this case, low saturated colors appear at locations with low uncertainties and the colors appear whitened or paled. Also, here it is possible to use a remap interval of uncertainty to avoid too paled effects. Using the Saturation component, the original predicted colors seem to be preserved better than when the Intensity is considered.

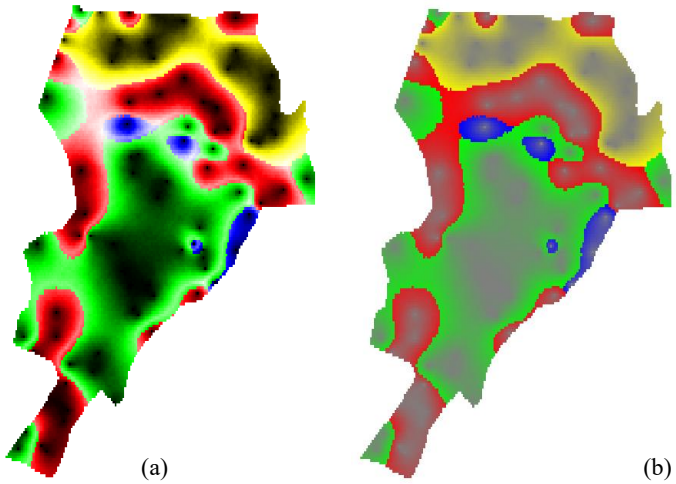

Figure 4: Fusion using IHS-RGB transformation replacing (a) the Intensity and (b) the Saturation by the Uncertainty map.

Moreover, the maps of Figure 4 can be rendered using the inverted uncertainty information. This can be done after applying an inverted linear function, mapping 0 to 254 and vice-versa, in the uncertainty map before the fusions. The results of using inverted uncertainties are shown in Figure 5 where the black and paled areas appear at the transition regions where the uncertainties are higher. These images keep the class colors, or saturate in white, where the uncertainties are lower.

Although the effectiveness of the above visualization methods has not yet been evaluated by a substantial number of users it suggests that the maps of Figures 4 and 5 allow one to have an integrated perception of both information, the predicted colors, or classes, and the uncertainties, mixed in the same map. Furthermore, these maps could be used as background of cartographic charts in order to enhance their final presentation, for example. The fusion maps can also be used as texture information for the 3D planar projection as presented in Figure 3.

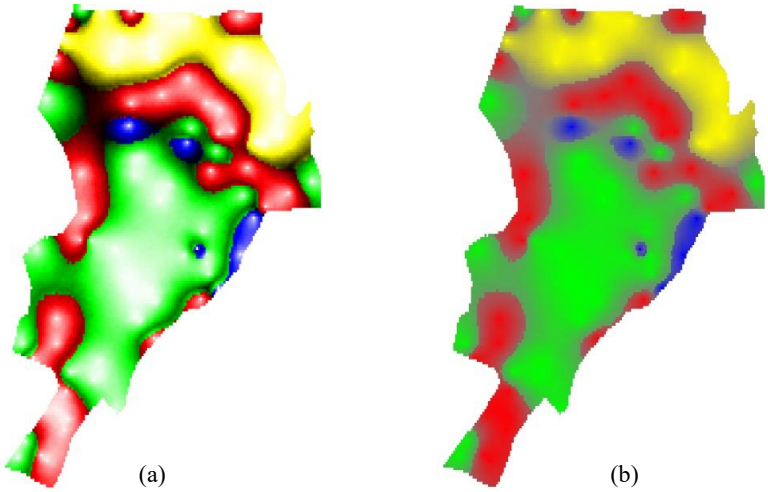

(a) (b)

Figure 5: Fusion using IHS-RGB transformation replacing (a) the Intensity and (b) the Saturation by the Inverted Uncertainty map.

6. Conclusions

This paper explored a geostatistical methodology for spatial modelling of categorical attributes that yield also the uncertainties related to the predictions. Furthermore, it presented different ways to visualize the predictions and their uncertainty information. The article showed also that the uncertainty can be visualized in a map separated from the map representing the spatial attribute. But sometimes it is interesting to integrate both information such as when the uncertainty is plotted using a 3D planar projection using the attribute data as the texture of the rendered figure. A more complex option is to use a fusion technique to create a unique map that presents the uncertainty mixed with the predictions. In this work, the RGB-IHS fusion technique was considered. The Hue was maintained as the original one while the Intensity or the Saturation component of the predicted information was replaced by the uncertainty information. After the reverse transformation, the RGB color composition showed maps where data and their uncertainties could be perceived in the same map. Besides, the resulting mixed maps can be used as backgrounds of cartographic charts and for planning actions on decision making activities, for example. In the future, we intend to explore similar methodology for spatial modelling of spatial continuous attributes and other fusion techniques.

Acknowledgements

Our thanks to the São Paulo Research Foundation FAPESP (www.fapesp.br/en/) by its financial support for this research work under the project grant number 15/24676-9.

References

Camara G., Souza R. C. M., Freitas U.M., Garrido J. (1996) “SPRING: Integrating remote sensing and GIS by object-oriented data modelling”, Computers & Graphics, 20:(3), p. 395-403.

Deutsch C. V. and Journel A. G. (1998) GSLIB: geostatistical software library and user's guide. Oxford University Press, New York, USA, 369p.

Felgueiras C. A., Monteiro A. M. V., Ortiz J. and Camargo E. C. G. (2015) "Improving Accuracy of Categorical Attribute Modelling with Indicator Simulation and Soft Information". In: Proceedings of the 13th International Conference on GeoComputation. University of Texas at Dallas, Richardson, Texas, USA, p. 25-31.

Foley J. D., vanDam A., Feiner S.K. and Hughes J.F. (1990). Computer Graphics: Principles and Practice. Second Edition, Addison-Wesley, Reading, 1174p.

Foody G. M. and Atkinson P. M. (2002) Uncertainty in Remote Sensing and GIS. London: Wiley Europe.

Goovaerts, P. (1997) Geostatistics for natural resources evaluation. Oxford University Press, NY, USA, 483p.

Goovaerts, P. (2001) "Geostatistical modelling of uncertainty in soil science", Geoderma, 103, p. 3–26.

Isaaks E. H. and Srivastava R. M. (1989) An Introduction to Applied Geostatistics. Oxford University Press, New York, USA. 561p.

Hengl T. (2003). Visualization of uncertainty using the HSI color model: computations with colors. 7th International Conference on GeoComputation (CD-ROM), University of Southhampton, Southhampton. pp. 8.

Kinkeldey, C., Mason, J., Klippel, A., & Schiewe, J. (2014). Evaluation of noise annotation lines: using noise to represent thematic uncertainty in maps. Cartography and Geographic Information Science, 41(5), 430-439,

Koo H., Chun Y., Griffith D. A. (2015) "Geovisualization of Attribute Uncertainty", In Proceedings of the 13th Int. Conference on GeoComputation, The University of Texas at Dallas, Richardson, Texas, USA, p. 230-236.

Newman W. M. and Sproull R. F. (1979) Principles of Interactive Computer Graphics, Second Edition, McGraw-Hill Inc., New York, 541p.

Pebesma E. J., K. de Jong, and D. Briggs. (2007) "Interactive visualization of uncertain spatial and spatiotemporal data under different scenarios: an air quality example", International Journal of Geographical Information Science, 21 (5), p. 515-527.

Senaratne, H., Gerharz, L., Pebesma, E., & Schwering, A. (2012). Usability of Spatio-Temporal Uncertainty Visualisation Methods. In J. Gensel, D. Josselin, & D. Vandenbroucke (Eds.), Bridging the Geographic Information Sciences: International AGILE'2012 Conference, Avignon (France), April, 24-27, 2012 (pp. 3-23). Berlin, Heidelberg: Springer Berlin Heidelberg.

Sun M. and Wong D. W. S. (2010) "Incorporating Data Quality Information in Mapping American Community Survey Data". Cartography and Geographic Information Science, 37, (4), p. 285–299

Tan M. and Chen J. (2008) "Visualization of uncertainty associated with spatial prediction of continuous variables using HSI color model: a case study of prediction of pH for topsoil in peri-urban Beijing, China". Journal of Forestry Research, 19 (4), p. 319-322